
Bullseye Polytope: A Scalable Clean-Label Poisoning Attack with Improved Transferability

Hojjat Aghakhani¹ Dongyu Meng¹ Yu-Xiang Wang¹ Christopher Kruegel¹ Giovanni Vigna¹

Abstract

A recent source of concern for the security of neural networks is the emergence of clean-label dataset poisoning attacks, wherein correctly labeled poisoned samples are injected in the training dataset. While these poisons look legitimate to the human observer, they contain malicious characteristics that trigger a targeted misclassification during inference. We propose a scalable and transferable clean-label attack, Bullseye Polytope, which creates poison images centered around the target image in the feature space. Bullseye Polytope improves the attack success rate of the current state-of-the-art by 26.75% in end-to-end training, while increasing attack speed by a factor of 12. We further extend Bullseye Polytope to a more practical attack model by including multiple images of the same object (e.g., from different angles) in crafting the poisoned samples. We demonstrate that this extension improves attack transferability by over 16% to unseen images (of the same object) without increasing the number of poisons.

1. Introduction

Machine-learning-based systems are being increasingly deployed in security-critical applications such as face recognition (Parkhi et al., 2015; Sun et al., 2014), fingerprint identification (Wang et al., 2014), cybersecurity (Suciu et al., 2018), as well as applications with high cost of failure such as autonomous driving (Chen et al., 2015). The existence of adversarial examples in deep neural networks has raised serious doubt on the security of these systems (Goodfellow et al., 2014; Biggio et al., 2013; Szegedy et al., 2013). In these evasion attacks (adversarial examples), a targeted input is perturbed by imperceptible amounts at test time in

order to avoid detection or trigger misclassification by a trained network. But neural networks are also vulnerable to malicious manipulation during the *training* process.

As neural networks often require large datasets for training, it is common practice to use training samples collected from other, often untrusted, sources (e.g., the Internet), and it is expensive to have these datasets carefully vetted. While neural networks are strong enough to learn powerful models in the presence of *natural* noises, they are vulnerable to carefully crafted malicious noise introduced deliberately by adversaries. In particular, gathering data from untrusted sources makes neural networks susceptible to *data poisoning attacks*, where an adversary injects data into the training set to manipulate or degrade the system performance. Unlike adversarial examples (Goodfellow et al., 2014; Biggio et al., 2013; Szegedy et al., 2013) and backdoor attacks (Chen et al., 2017a; Turner et al., 2018; Liu et al., 2017), data poisoning attacks do not modify the target sample during inference.

This work focuses on *clean-label poisoning attacks*, a branch of poisoning attacks wherein the attacker does not have any control over the labeling process. In this threat model, the poisoned samples are created by introducing imperceptible yet malicious alterations that will result in model misbehavior in response to specific target inputs. These perturbations are small enough to maintain the original images' labels in the eye of a domain expert. The stealth of the attack increases the success rate in real-world scenarios compared to other types of data poisoning attacks, as the poisoned data (1) will not be identified by human labelers, and (2) does not degrade test accuracy except for misclassification of particular target examples.

Clean-label poisoning attack on *transfer learning* was first studied in the *white-box* setting (Shafahi et al., 2018) where the attacker has complete knowledge of the pre-trained network ϕ that the victim employs to either (1) extract features for training a (linear) classifier (*linear transfer learning*) or (2) fine-tunes on a similar task (*end-to-end training*). The *Feature Collision* attack (Shafahi et al., 2018) selects a base image x_b from the (intended) misclassification class and creates a poison sample, x_p , by adding small (bounded) adversarial perturbations to x_b such that x_p is similar to the

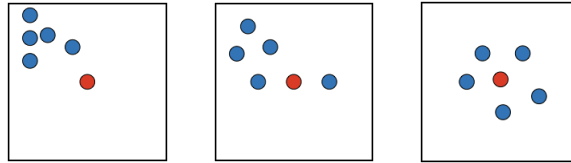
¹University of California, Santa Barbara. Correspondence to: Hojjat Aghakhani <hojjat@cs.ucsb.edu>, Dongyu Meng <dmeng@cs.ucsb.edu>, Yu-Xiang Wang <yuxiangw@cs.ucsb.edu>, Christopher Kruegel <chris@cs.ucsb.edu>, Giovanni Vigna <vigna@cs.ucsb.edu>.

target image in the feature space created by ϕ . Feature Collision tends to fail in gray-box or black-box settings where the feature extractor ϕ is unknown to the attacker. To mitigate limitations of Feature Collision, *Convex Polytope* was proposed (Zhu et al., 2019), which, instead of finding poisons close to the target, finds a set of poisons that form a convex polytope around it, hoping that the target’s feature vector lies within (or at least close to) this “attack zone” in the victim’s feature space. This is a far more relaxed condition than what is enforced by Feature Collision, as it enables the poisons to lie much further away from the target. Convex Polytope relies on the fact that every linear classifier that classifies a set of points into label l will also classify every point in the convex hull of these points as label l .

The most important advantage of Convex Polytope to Feature Collision is improved transferability of the targeted misclassification to the victim’s (fine-tuned) classifier, where the feature extractor ϕ is unknown to the attacker. However, as we show here, the target feature vector in Convex Polytope tends to be close to the boundary of the attack zone, potentially hampering the transferability of the attack. Another major downside of Convex Polytope is that it is very slow. For example, crafting a set of five poisons for a single target takes ~ 17 hours on average.¹ This poses a serious bottleneck for future research, especially for designing defenses against this class of attacks.

To address these limitations, we propose Bullseye Polytope, which modifies the constraints of Convex Polytope such that the target is pushed toward the “center” of the attack zone (i.e., convex hull of poisons). The geometrical comparison of Bullseye Polytope and Convex Polytope is shown in Figure 1. Bullseye Polytope improves both the transferability and speed of convergence compared to the state of the art. When the victim adopts linear transfer learning, our method improves the attack transferability by 7.44% on average, while being 11x faster. In end-to-end training, Bullseye Polytope outperforms Convex Polytope by 26.75% in terms of attack success rate, while being 12x faster. In a more restricted threat model where the adversary has limited knowledge of the training set of the victim’s feature extractor ϕ , Bullseye Polytope increases attack success rate in linear transfer learning by 9.27%.

We also extend Bullseye Polytope to a more *practical* threat model. Current clean-label poisoning attacks are designed to target only one image at a time, rendering them ineffective against unpredictable variations in real-world image acquisition. Such attacks disregard the following major point: to succeed in real-world scenarios, the attack needs to cope with a spectrum of test inputs. By including a larger number of target images (of the same object) when crafting the poisons, we are able to obtain attack transferability of



(a) Original images. (b) Convex Polytope (c) Bullseye Polytope

Figure 1. Simplified representation of poisons crafted by Convex Polytope and Bullseye Polytope in two-dimensional feature space. Blue circles are poisons and the red circle is the target. Convex Polytope moves poisons until the target is inside their convex hull, making no further refinements to move the target away from the polytope boundary, whereas Bullseye Polytope pushes the target toward the polytope center.

49.56% against *unseen* images (of the same object), without increasing the number of poisons. This is over 16% improvement compared to single-target mode when testing against the same set of images (in linear transfer learning).

Our experiments show that Bullseye Polytope is not only more successful than current state-of-the-art of clean-label poisoning attacks, but, perhaps more importantly, it is an order of magnitude faster. When building future defenses against this class of attacks, being able to run the attack in a short time makes a huge difference. In this light, our work not only improves the state of the art, but also facilitates future research by severely cutting down computing time. The source code of all experiments can be found at github.com/ucsb-seclab/BullseyePoison.

2. Threat Model

Similar to the clean-label poisoning attacks proposed by (Shafahi et al., 2018) and (Zhu et al., 2019), in our setting, the attacker injects a small number of perturbed samples, or *poisons*, into the training set of the victim. The attacker does not have any control over the labeling process, and the poisons are made by imperceptible changes to the original samples. Therefore, the poisons will maintain their malicious characteristics, despite being labeled correctly by human experts. The attacker has no access to the victim model, and only has knowledge of the victim’s training set distribution (black-box setting). In the gray-box setting, the victim network’s architecture is also known. The attacker uses a similar training set for training *substitute networks*, which will be used to craft poisons with the hope that they are transferable to the (unseen) victim’s network.

To compare to the latest clean-label attacks (Zhu et al., 2019), we consider two transfer learning approaches that the victim may adopt, linear transfer learning and end-to-end training. Transfer learning is a general approach where a model trained for one task is reused as part of a different model for a second task. In linear transfer learning, a pre-trained but **frozen** network acts as a feature extractor

¹Graphics cards are used for all experiments.

ϕ , and an application-specific **linear** classifier is fine-tuned on the features extracted via ϕ . Linear transfer learning is shown to be a common practice, as it obtains high-quality models without incurring the cost of training a model from scratch (Gu et al., 2017). In end-to-end training, the feature extractor and linear classifier are trained jointly, therefore the feature extractor is altered after fine-tuning. Unless explicitly stated, by “attack transferability” we mean the transferability of the targeted misclassification to the victim’s (fine-tuned) classifier where the victim’s feature extractor ϕ is unknown, but the training set that is used for ϕ is known to the attacker. We further evaluate the poisoning attacks in a more limited setting where the adversary has no or partial knowledge of the *training set* of ϕ .

Poisoning attacks may aim to cause misclassification on one or multiple inputs. To succeed on real-world applications such as face recognition models in surveillance systems, the attack needs to cope with a spectrum of test inputs. To the best of our knowledge, current clean-label poisoning attacks only work with one image at a time, rendering them ineffective in more realistic attack scenarios. Bullseye Polytope overcomes this limitation by accelerating the Convex Polytope attack and improving transferability by incorporating multiple targets into the poisoning process.

3. Related Work

A well-studied portion of data poisoning attacks aim to use malicious data to degrade the test accuracy of the model (Nelson et al., 2008; Biggio et al., 2012; Xiao et al., 2012; Mei & Zhu, 2015; Burkard & Lagesse, 2017). While such attacks are shown to be successful, they are easy to detect, as the performance of the model can always be assessed by evaluating on a private, trusted set of samples. Another important branch of data poisoning attacks, known as *backdoor attacks* (Gu et al., 2017), aim to imprint a small number of training examples with a specific pattern (*trigger*) and change their labels to the target label. During inference, the attacker achieves misclassification by injecting the trigger into targeted examples. This strategy is shown to be effective, however, it relies on the assumption that the poisoned data will not be inspected by any filtering process, human or automated. In general, similar to evasion attacks, these attacks present the following shortcoming: they require the modification of test samples during inference to enable misclassification.

The first clean-label poisoning attack is Feature Collision (Shafahi et al., 2018), which mainly targets linear transfer learning, where the adversary has complete knowledge of the feature extractor network ϕ employed by the victim. To trigger misclassification for a specific target image x_t , Feature Collision selects a base image x_b from the targeted class and crafts a poison sample x_p by adding small

(bounded) adversarial perturbations to x_b such that x_p is similar to the target image in the feature space defined by ϕ . A linear classifier that is trained on the features of a dataset containing x_p will identify x_t as the targeted class, since $\phi(x_t) \approx \phi(x_p)$. Feature Collision suffers from two major problems (Zhu et al., 2019); first, it tends to fail in black-box settings, and second, in some cases, noticeable patterns of the target image appear in the crafted poisons.

To mitigate such limitations, (Zhu et al., 2019) proposed the Convex Polytope attack, which crafts a set of poisons that contain the target’s feature vector within their convex hull. Based on this characteristic, if the victim’s linear classifier associates the poisons with the targeted class, it will label any point inside their convex hull as the targeted class. Convex Polytope creates a larger “attack zone” in the feature space, thus increasing the chance of transferability, as argued by the authors. In particular, it outperforms Feature Collision by 20% on average in terms of attack success rate, while introducing less obvious patterns in poisons. As we will show in Section 6, Convex Polytope suffers from two shortcomings. (1) *Speed*: Convex Polytope is significantly slow. For example, crafting a set of five poisons for a single target takes ~ 17 hours on average. (2) *Robustness*: The target’s feature vector tends to be close to the boundary of the polytope formed by the poisons, leaving untapped the full potential for attack transferability.

We design Bullseye Polytope based on the insight that by predetermining the relative position of the target with respect to the poisons’ convex hull, we can significantly speed up the attack while also improving resiliency to unseen networks. Bullseye Polytope accelerates poison construction by 10-36x compared to Convex Polytope across experiments. The generated poisons also provide higher attack success rates in both transfer learning setups. We further improve the robustness of Bullseye Polytope by incorporating multiple images of a target object. We demonstrate that the resulting attack is effective on *unseen* images of the target while maintaining good baseline test accuracy on non-targeted images. This is a vitally important feature for practical implementations on real-world systems. To the best of our knowledge, Bullseye Polytope is the first clean-label poisoning attack being proposed for a multi-target threat model.

4. Background

In this section, we describe the Convex Polytope attack (Zhu et al., 2019) against transfer learning. We employ the same notations used in their paper. Convex Polytope exploits the following mathematical guarantee: if a linear classifier classifies a set of poisons into the same class, l_p , it will label any input x_t whose feature vector, $\phi(x_t)$, lies in the convex polytope formed by the poisons in the feature space as the same class l_p . Therefore, in the black-box setting, as long

as x_t lies inside this region in the (unknown) feature space created by the victim model, the target will be classified with the same label l_p . In particular, Convex Polytope solves the following optimization problem:

$$\begin{aligned} & \underset{\{c^{(i)}\}, \{x_p^{(j)}\}}{\text{minimize}} && \frac{1}{2} \sum_{i=1}^m \frac{\left\| \phi^{(i)}(x_t) - \sum_{j=1}^k c_j^{(i)} \phi^{(i)}(x_p^{(j)}) \right\|^2}{\left\| \phi^{(i)}(x_t) \right\|^2} \\ & \text{subject to} && \sum_{j=1}^k c_j^{(i)} = 1, c_j^{(i)} \geq 0, \forall i, j, \\ & && \left\| x_p^{(j)} - x_b^{(j)} \right\|_{\infty} \leq \epsilon, \forall j, \end{aligned} \quad (1)$$

where $x_b^{(j)}$ is the original image of the j -th poison, and ϵ determines the maximum allowed perturbation. Notice that Eq. 1 finds a set of poisons $\{x_p^{(j)}\}_{j=1}^k$ such that the target lies inside, or at least close to, the convex hull of the poisons in the feature space defined by m substitute networks $\{\phi^{(i)}\}_{i=1}^m$. In the i -th substitute network, the target feature vector $\phi^{(i)}(x_t)$ is ideally a convex combination of the feature vectors of poison images, i.e., $\phi^{(i)}(x_t) = \sum_{j=1}^k c_j^{(i)} \phi^{(i)}(x_p^{(j)})$, where $c_j^{(i)}$ determines the coefficient of the j -th poison in substitute network i . To solve the non-convex and constrained problem (Eq. 1), Convex Polytope takes the following steps in each iteration:

1. By freezing $\{\phi(x_p^{(j)})\}_{j=1}^k$, use forward-backward splitting (Goldstein et al., 2014) to find the optimal sets of coefficients for each individual network $\{c^{(i)}\}$.
2. Given the optimal $\{c^{(i)}\}$, take one gradient step to optimize $\{\phi(x_p^{(j)})\}_{j=1}^k$.
3. Clip $\{x_p^{(j)}\}_{j=1}^k$ to the ϵ -ball around the clean base images $\{x_b^{(j)}\}_{j=1}^k$.

With $\epsilon = 0.1$, Convex Polytope repeats these steps for 4,000 iterations to find the optimal set of poisons.

Dropout Randomization. Attack transferability improves when we increase the number of substitute networks for crafting poisons. However, it is impractical to ensemble a large number of networks due to memory and time constraints. For this reason, Convex Polytope leverages dropout randomization when crafting poisons to avoid overfitting to the feature spaces of any particular substitute network.

Ensemble Feature Collision. To evaluate the effectiveness of the Convex Polytope attack, (Zhu et al., 2019) developed an ensemble version of Feature Collision (Shafahi et al., 2018) to craft *multiple* poisons instead of one.² They

²This was originally practiced by the authors of (Shafahi et al., 2018) to improve performance in the end-to-end training scenario.

further used this ensemble version as a benchmark. The corresponding loss function is defined as:

$$\mathcal{L}_{FC} = \sum_{i=1}^m \sum_{j=1}^k \frac{\left\| \phi^{(i)}(x_p^{(j)}) - \phi^{(i)}(x_t) \right\|^2}{\left\| \phi^{(i)}(x_t) \right\|^2}. \quad (2)$$

They argue that unlike Feature Collision, Convex Polytope’s loss function (Eq. 1) allows the poisons to lie further away from the target. This (1) prevents poisons from showing apparent patterns resembling the target, and (2) improves transferability, as the convex polytope creates a larger space than the ball generated by the Feature Collision attack. Experiments showed that Convex Polytope outperforms Feature Collision, especially in black-box settings.

It should be noted that, contrary to what is stated in (Zhu et al., 2019), the Ensemble Feature Collision attack objective described by Eq. 2 is not a special case of Eq. 1 (when the coefficients are set to $\frac{1}{k}$), rather, it optimizes completely decoupled objectives for different poisons. While centering the target between poisons allows more flexibility in poison locations, Eq. 2 pushes all poisons close to the target which has the same drawbacks of collision attacks, namely, perceptible patterns showing up in poison images and limited transferability. By exploiting this approach of centering, we show that Bullseye Polytope improves both attack transferability and scalability.

Scalability Issue of Convex Polytope. We observed that when using 18 substitute networks, solving Eq. 1 for five poisons (in 4,000 iterations) takes ~ 17 hours on average.³ Of this time, step one alone takes ~ 15 hours. We list the detailed algorithm of step one in the supplementary material (Algorithm 1). Among the listing, we noticed two major time-consuming operations: (1) The condition that checks whether the new coefficients result in a smaller loss than what we have for the old coefficients. This condition is checked in every iteration of coefficients optimization. (2) The projection onto the probability simplex, which happens when the new coefficients satisfy the above condition. While we believe that there is room for improvement in the implementation of this algorithm (possibly resulting in slightly higher loss), e.g., by checking the condition every few steps rather than each step, we did not make any such changes in order to avoid degradation of the attack success rate, and allow for a fair comparison.

5. Bullseye Polytope

To tackle the scalability and transferability issue of Convex Polytope, we propose Bullseye Polytope. Instead of searching for coefficients by optimization, which is neither efficient nor effective, Bullseye Polytope *predetermines* the

³With the same setting in the original paper.

coefficients before poison crafting. More specifically, Bullseye Polytope sets the coefficients to $\frac{1}{k}$ to enforce that the target resides close to the “center” of the polytope formed by poisons in feature space.⁴ Bullseye Polytope then solves this special case of the search formalization. With the Convex Polytope attack, as soon as the target crosses the boundary into the interior of the convex polytope of poisons, there is no incentive to refine further and move the target deeper inside the attack space (Figure 1). Therefore, Convex Polytope often produces poisons that define a polytope whose border is close to the target. This proximity to the boundary reduces robustness and limits generalization. Bullseye Polytope, on the other hand, improves attack transferability by effectively pushing the target away from the polytope border and toward its center. Also, by precluding the most time-consuming step of computing coefficients, Bullseye Polytope is an order of magnitude faster than Convex Polytope. Formally, by setting the coefficients to $\frac{1}{k}$, Bullseye Polytope solves the following optimization problem for single-target mode.

$$\begin{aligned} \underset{\{x_p^{(j)}\}}{\text{minimize}} \quad & \frac{1}{2} \sum_{i=1}^m \frac{\left\| \phi^{(i)}(x_t) - \frac{1}{k} \sum_{j=1}^k \phi^{(i)}(x_p^{(j)}) \right\|^2}{\left\| \phi^{(i)}(x_t) \right\|^2} \\ & \left\| x_p^{(j)} - x_b^{(j)} \right\|_{\infty} \leq \epsilon, \forall j. \end{aligned} \quad (3)$$

Improved Transferability via Multi-Draw Dropout.

Similar to Convex Polytope, we found that activating dropout when crafting poisons improves transferability. With dropout, the substitute network $\phi^{(i)}$ provides a different feature vector for the same poison each time. This randomization was observed to result in much higher variance in the (training) loss of Eq. 3 compared to that of Eq. 1. Since the solution space of Eq. 3 is much more restrictive than Eq. 1, and moves around for different realizations of dropout, gradient descent has a harder time converging for Eq. 3. To tackle this problem, we optimize over the average of multiple draws. In each iteration, we compute the feature vector of poisons R times for each network, and use the mean feature vectors in optimizing Eq. 3. Of course, increasing R results in higher attack execution time, but even a modest choice of $R = 3$ is enough to achieve a 8.5% higher attack success rate compared to when $R = 1$ for end-to-end training. It should be noted that, even in this case, Bullseye Polytope is 12 times faster than Convex Polytope. We note here that the same technique is not applicable to Convex Polytope as it is already very slow.

Multi-target Mode. In real-world applications, the image acquisition process introduces variations to captured images. These variations include, but are not limited to, lighting

⁴Our notion of the center coincides with the *center of mass* of the poison set.

conditions and observation angle. In this light, to generate poisons that are likely to be useful in practice, we craft poisons that trigger the misclassification for all images captured for the same *object* (target) by creating poisons based on a set of different images of that object.

To craft a more generalizable attack, we consider a set of N_K target images of the same object and simply compute the average of their target feature vectors, ν , and perform Bullseye Polytope on ν . The intuition behind this approach follows from the fact that (1) the pretrained network is a powerful feature extractor, therefore, images of the same object will be close to each other in this space, and (2) the mean feature vector contains the most significant component of the feature-space embedding of that object. We expect centering poisons around ν to increase the chances of unseen images (of the same object) falling inside the “attack zone.” In Section 6.2, we show the effectiveness of this technique on unseen target images.

End-to-End Training

In end-to-end training, the victim retrains both the feature extractor and the linear classifier. After fine-tuning the whole network on the poisoned dataset, the feature space is no longer the same as before. Therefore, even in the white-box setting, the target feature vector may no longer reside in the convex polytope. In gray-box or black-box settings, such a change in the feature space makes Convex Polytope even harder to transfer. To tackle this issue, as inspired by Convex Polytope, we jointly apply Bullseye Polytope to multiple layers of the network. Bullseye Polytope crafts the poisons such that the feature space created by each layer of the network satisfies Eq. 3. Indeed, this adds to the complexity of the problem, which is especially problematic for the Convex Polytope attack.

6. Experiments

In this section, we first evaluate Bullseye Polytope (*BP*), against Convex Polytope (*CP*) with the substitute networks and datasets used in (Zhu et al., 2019) in single-target mode. We then show the transferability of Bullseye Polytope on unseen images of the target object by testing on multi-target mode. BP-3x and BP-5x represent the case where multi-draw dropout is enabled for Bullseye Polytope, with R set to 3 and 5, respectively. Unless stated otherwise, we use the exact same settings as used by (Zhu et al., 2019) to provide a fair comparison.

6.1. Single-target Mode

Datasets. We use the CIFAR-10 dataset in single-target mode. If not explicitly stated, all the substitute and victim models are trained using the first 4,800 images from each of the 10 classes (a total of 48,000 images). In all experiments, we use the standard test set from CIFAR-10 to evaluate *base-*

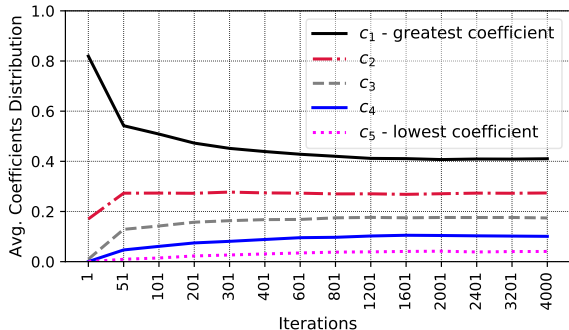


Figure 2. Distribution of coefficients (averaged over all targets and victim networks). The coefficients are sorted, c_1 denotes the highest coefficient and c_5 denotes the lowest coefficient.

line test accuracy⁵ of the poisoned models, and compare them with the ordinary models (trained without poisons). Attack targets, base images of poisons, and victim’s fine-tuning set come from the remaining 2,000 images of the training set. We assume victim models are fine-tuned on a training set consisting of the first 50 images from each class, i.e., the *fine-tuning dataset*, containing a total of 500 images. The authors of (Zhu et al., 2019) randomly selected ship as the target image class, and frog as the misclassification class. We follow this setting for comparison fairness. Specifically, the attacker crafts clean-label poisons from ship images to cause a particular frog image to be misclassified as a ship. We craft the poison images $x_p^{(j)}$ from the first five images of the ship class in the fine-tuning dataset. We evaluate CP and BP on the next 50 images of the frog class to collect statistics. It should be noted that target images, training set, and fine-tuning set are mutually exclusive subsets. For all experiments, we set an ℓ_∞ budget of $\epsilon = 0.1$.

6.1.1. LINEAR TRANSFER LEARNING

Attack Settings. For substitute networks, we use SENet18 (Hu et al., 2018), ResNet50 (He et al., 2016), ResNeXt29-2x64d (Xie et al., 2017), DPN92 (Chen et al., 2017b), MobileNetV2 (Sandler et al., 2018), and GoogLeNet (Szegedy et al., 2015). Each of these substitute network architectures is trained with dropout probabilities of 0.2, 0.25 and 0.3, which results in a total of 18 substitute models. To evaluate the attacks under gray-box settings, we use the aforementioned architectures (although trained with a different random seed). To test under black-box settings, we use two new architectures, ResNet18 (He et al., 2016) and DenseNet121 (Huang et al., 2017). Dropout remains activated when crafting the poisons to improve attack transferability. However, all eight victim models are trained without dropout, and dropout is disabled when evaluating on them. We perform both CP and BP attacks for 4,000 iterations with the same hyperparameters used by CP. The only

⁵Accuracy on non-targeted images.

difference is that BP forces the coefficients to be uniform, i.e., $c_j^{(i)} = \frac{1}{5}$. We use Adam (Kingma & Ba, 2014) with a learning rate of 0.1 to fine-tune the victim models on the poisoned dataset for 60 epochs.

Attack Success Rate. Figure 6 shows the progress of CP and BP over the number of iterations of the attack. For each individual victim network, the attack progress of CP and BP is provided in supplementary material (Figure 13). As Figure 3a shows, Bullseye Polytope outperforms CP on average (over victim models), and converges faster. In particular, on average over all iterations, BP-3x and BP-5x demonstrate 7.44% and 8.38% higher attack success rates than CP. Both CP and BP hardly affect the baseline test accuracy of models (Figure 5a).

Attack Execution Time. BP is almost 21 times faster than CP, as it excludes the computation-heavy step of optimizing the coefficients. Figure 4a shows the attack execution time based on the number of iterations. Running CP for 4,000 iterations takes 1,002 minutes on average, while BP takes only 47 minutes. BP-3x and BP-5x take 88 and 141 minutes respectively. It is worth noting that BP needs fewer iterations than CP to achieve the same attack success rate (Figure 6).

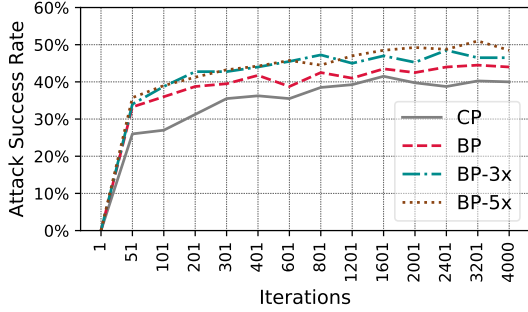
6.1.2. END-TO-END TRAINING

In end-to-end training, the victim feature extractor is changed after the fine-tuning process, which results in a (slightly) different feature space. This causes the conventional CP attack to have poor transferability of less than 5% when the entire network is retrained (Zhu et al., 2019). To tackle this problem, (Zhu et al., 2019) extends CP to create convex polytopes in different layers of the substitute models. We follow the same strategy for BP.

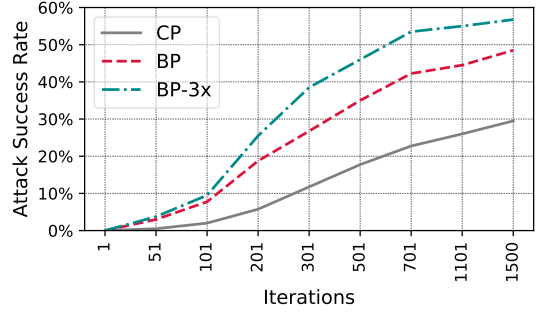
Attack Settings. We perform CP and BP for only 1,500 iterations due to time and resource constraints. For substitute networks, we use SENet18, ResNet50, ResNeXt29-2x64d, and DPN92, with dropout values of 0.2, 0.25, and 0.3, which results in a total of 12 substitute models. For gray-box testing, we evaluate attack transferability against all four aforementioned architectures. MobileNetV2, GoogLeNet, ResNet18, and DenseNet121 are used as victim networks in the black-box setting. We use Adam (Kingma & Ba, 2014) with a learning rate of 10^{-4} to fine-tune the victim models on the poisoned dataset for 60 epochs.

Attack Success Rate. Similar to what we observed for linear transfer learning (but with a wider margin), BP presents higher attack transferability than CP, especially in the black-box setting. Here we report attack success rates after 1,500 iterations. BP and BP-3x improve attack transferability by 18.25% and 26.75% (Figure 3b). Figure 14 in supplementary material shows the attack success rates against each

Bullseye Polytope: A Scalable Clean-Label Poisoning Attack with Improved Transferability

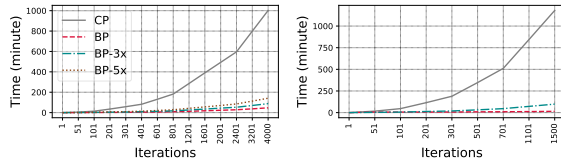


(a) Linear transfer learning



(b) End-to-end training

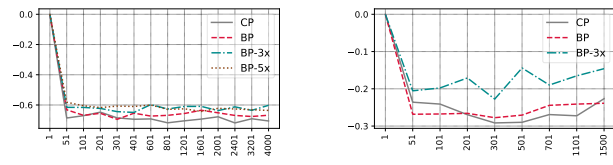
Figure 3. Attack success rates of CP, BP, BP-3x and BP-5x, averaged over all eight victim models.



(a) Linear transfer learning

(b) End-to-end training

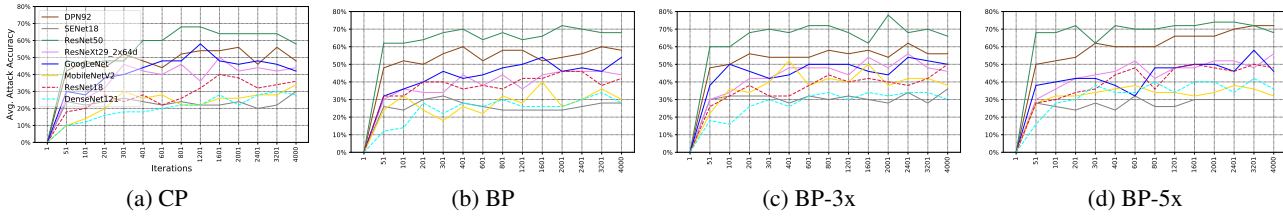
Figure 4. Attack execution time.



(a) Linear transfer learning

(b) End-to-end training

Figure 5. Average change in baseline test accuracy of models.



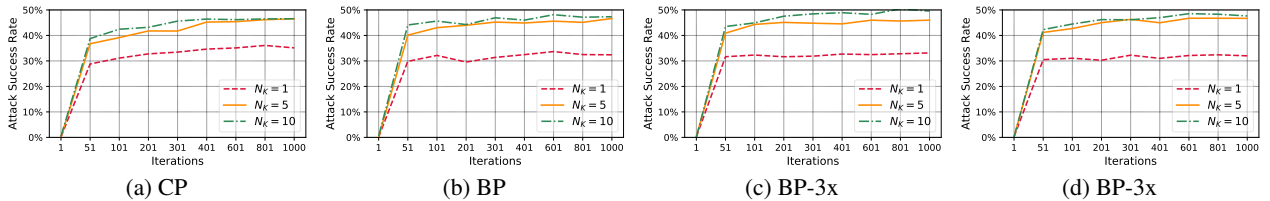
(a) CP

(b) BP

(c) BP-3x

(d) BP-5x

Figure 6. Linear transfer learning - success rates of CP, BP, BP-3x and BP-5x on victim models. Notice ResNet 18 and DenseNet 121 are the black-box setting.



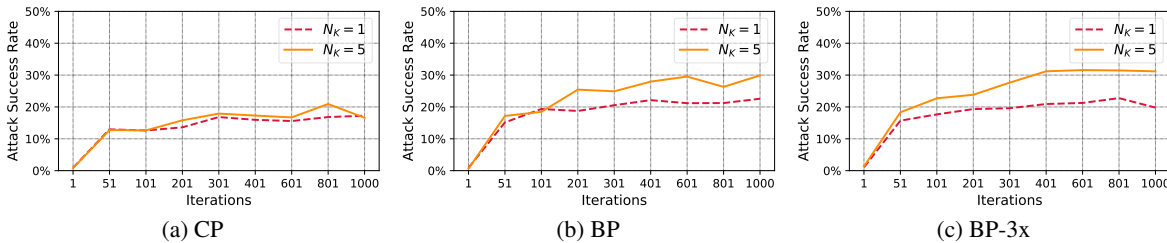
(a) CP

(b) BP

(c) BP-3x

(d) BP-5x

Figure 7. Attack transferability to unseen angles against linear transfer learning.



(a) CP

(b) BP

(c) BP-3x

Figure 8. Attack transferability to unseen angles for BP and BP-3x (averaged over all eight victim models).

individual victim model. BP and BP-3x have 10-30% and 10-50% higher attack transferability than CP, respectively (except against GoogLeNet). Poor transferability against GoogLeNet is also reported for CP (Zhu et al., 2019). Since the GoogLeNet architecture differs significantly from the substitute models, it is, therefore, more difficult for the “attack zone” to survive end-to-end training. For other black-box models (MobileNetV2, ResNet18, and DenseNet121), BP and BP-3x improve attack transferability by $\sim 18\%$ and $\sim 24\%$ respectively. Both CP and BP have hardly any effect on the baseline test accuracy of models (Figure 5b).

Attack Execution Time. Figure 4b shows attack execution time. While BP and BP-3x take 15 and 98 minutes, CP takes 1,180 minutes, which is 36x slower than BP.

6.1.3. TRANSFERABILITY TO UNSEEN TRAINING SETS

Until now, we have assumed that the substitute models are trained on the same training set (Ψ) on which the victim’s feature extractor network is trained. In this section, we evaluate CP and BP using substitute models that are trained on a training set which has (1) **zero** or (2) **50%** overlap with Ψ . Such a setting is more realistic compared to when the attacker has complete knowledge of Ψ .

Attack Settings. We use the same setting as in linear transfer learning except for the following changes. We train the victim models on the first 2,400 images of each class. In the zero overlap setting, substitute models are trained on samples indexed from 2,401 to 4,800 per each class. For the 50% overlap setting, we train all substitute models on samples indexed from 1,201 to 3,600 for each class.

Attack Success Rate. Figure 9 shows attack success rates (averaged over victims) for both zero overlap and 50% overlap setups. When we have 50% overlap, BP, BP-3x, and BP-5x demonstrate 5.82%, 8.56%, and 9.27% higher attack success rates compared to CP (on average over all iterations), with BP converging significantly faster than CP. For the zero overlap setup, BP provides hardly any improvement over CP. They both achieve much lower attack success rates of 20-25%. It should be noted that the zero overlap scenario is much more restricted than what is usually assumed in threat models of poisoning attacks. The victim’s network, training set, and even the fine-tuning training set (except, of course, the poisoned samples) are all unseen to the adversary. CP, BP, BP-3x, and BP-5x hardly affect the baseline test accuracy of models (Figure 18 in supplementary).

6.1.4. EFFECTIVENESS OF THE BULLSEYE IDEA

We have argued that the effectiveness (robustness and transferability) of BP stems from the fact that predetermining the convex coefficients as uniform weights draws the target

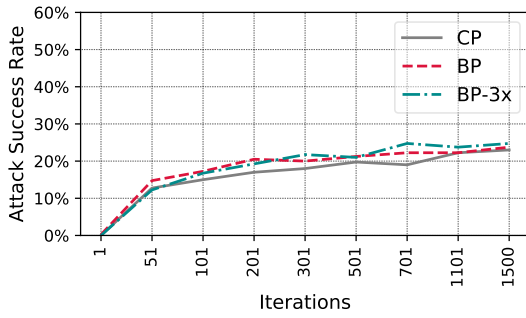
to the “center” of the attack zone, increasing its distance from the poison polytope boundary. In order to evaluate this claim quantitatively, we run the attack with different sets of *nonuniform* coefficients, to see if the improvement is truly due to target centering (i.e., the “bullseye” idea) or simply from “fixing” the coefficients instead of searching for them.

We evaluate BP against nine alternatives $\{BP'_t\}_{t=1}^9$, each with a different set of positive predefined coefficients that satisfy $\sum_{j=1}^k c_j = 1$. Figure 10 depicts a geometrical example for each set (sorted from left to right based on the entropy of the coefficient vector), with BP having the highest possible entropy of $\log_2 5 \simeq 2.32$. As Figure 11 shows, variations of BP with higher coefficient entropy generally demonstrate higher attack success rates compared to those with smaller entropy, especially in the black-box setting. This finding indicates that predetermining the coefficients to uniform weights (BP) is preferable to simply fixing them to some other plausible values. This backs our intuition behind BP that the further the target is from the polytope boundary, the lower its chances of jumping out of the attack zone in the victim’s feature space. In fact, the average entropy of coefficients in CP roughly converges to 1.70, which means the coefficient distribution is more skewed with some poisons having a relatively small contribution to the attack. Figure 2 shows the mean values of the (sorted) coefficients to provide a sense of the coefficient distributions produced by CP.

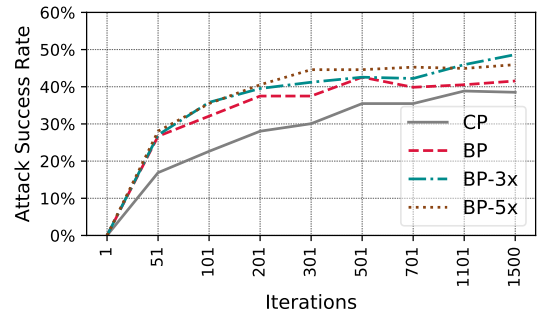
6.2. Multi-Target Mode

We now consider a more realistic setting where the target *object* is known but there is unpredictable variability in the target *image* at test time (e.g., unknown observation angle, lighting, etc.). This is the first attempt at crafting a *clean-label* and *training-time* dataset poisoning attack that is effective on multiple (unseen) images of the target object at test time. To this end, we consider a slight variation of Bullseye Polytope that takes multiple images of the target object (capturing as much observation variability as possible) and performs Bullseye Polytope on the averages of their feature vectors in all substitute networks.

Targets’ Dataset. We use the Multi-View Car Dataset (Ozuysal et al., 2009), which contains images from 20 different cars as they are rotated by 360 degrees at increments of 3-4 degrees. Multi-View Car Dataset contains a different distribution of images compared to CIFAR-10, therefore we expect to see lower test accuracy when testing the substitute models on this dataset. Out of all 20 cars, the substitute models present an accuracy of over 90% for 14 of the cars. We perform the attacks only for these 14 cars to get a lower-bound estimation of the performance of our attack, as for the other targets the models are more vulnerable, and thus easier to trick. We use the same settings and parameters as single-target mode.



(a) Zero overlap



(b) 50% overlap

Figure 9. Comparison of CP, BP, and BP-3x in linear transfer learning, with zero and 50% overlap between training sets of the substitute networks and the victim’s network.

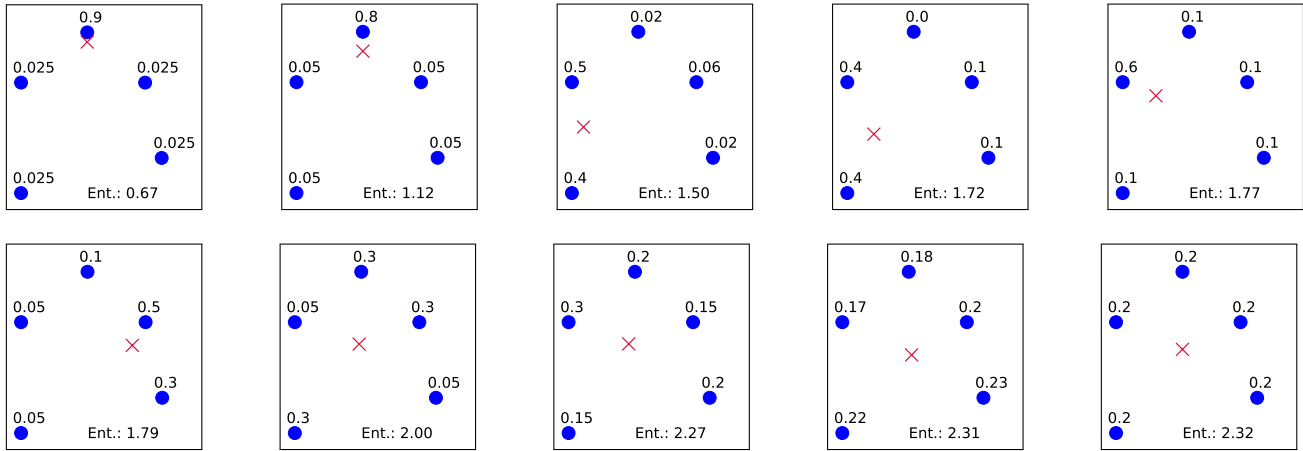
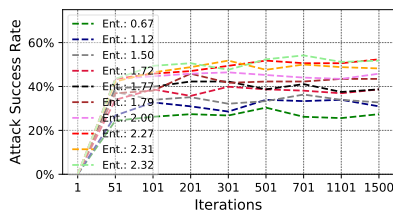
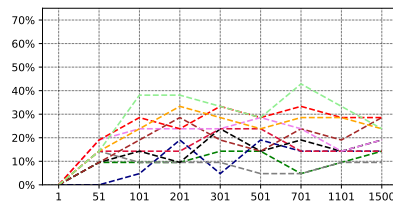


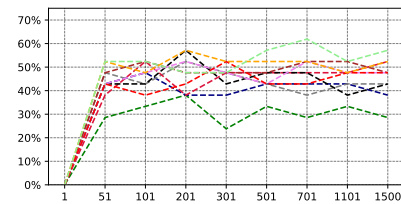
Figure 10. Nine alternatives of Bullseye Polytope with different sets of nonuniform coefficients. The blue circles are poisons with their coefficients written next to them, and the red cross is the target. The entropy of the coefficients increases from left to right. Note that the bottom right represents BP.



(a) Averaged over all eight victim models



(b) DenseNet121



(c) ResNet18

Figure 11. Comparison between BP and the other nine alternatives described at Figure 10.

We evaluate both CP and BP setting the number of target images, N_K , to 1, 5, and 10, in order to verify the effect of N_K on the attack robustness against unseen angles. Note that when $N_K = 1$, the attack is in single-target mode. To select the N_K target images for poison crafting, we take one image every $\frac{360}{N_K}$ degree rotation of the target car. Figure 7 and Figure 8 show the attack success rates against **unseen** images. In linear transfer learning, using five targets instead of one improves attack robustness against unseen angles by over 16%. For end-to-end training, BP-3x demonstrates an improvement of 12%. When $N_K = 5$, we observed that BP achieves 14% higher attack success rate compared to CP, while being 59x faster. We note that the total number of poisons crafted for multi-target attacks is the same as single-target mode (i.e., 5).

7. Conclusions

In this work, we present a scalable and transferable clean-label poisoning attack, Bullseye Polytope, for transfer learning. Bullseye Polytope searches for poisons that create, in the feature space, a convex polytope around the target image, ensuring that a linear classifier that trains on the poisoned dataset will classify the target into the poison class. By predetermining the relative position of the target and the polytope, Bullseye Polytope achieves 10-36x faster poison generation compared to the state-of-the-art attack, Convex Polytope. By driving the polytope center close to the target, Bullseye Polytope outperforms Convex Polytope’s attack success rate by 7.44% and 26.75% for linear transfer learning and end-to-end training, respectively. Furthermore, by including multiple images of the same target object when crafting the poisons, Bullseye Polytope shows attack transferability of 49.56% against *unseen* images (of the same object). This is 16% improvement compared to single-target mode when testing against the same set of images without increasing the number of poisons.

References

- Biggio, B., Nelson, B., and Laskov, P. Poisoning attacks against support vector machines. *arXiv preprint arXiv:1206.6389*, 2012.
- Biggio, B., Corona, I., Maiorca, D., Nelson, B., Šrndić, N., Laskov, P., Giacinto, G., and Roli, F. Evasion attacks against machine learning at test time. In *Joint European conference on machine learning and knowledge discovery in databases*, pp. 387–402. Springer, 2013.
- Burkard, C. and Lagesse, B. Analysis of causative attacks against svms learning from data streams. In *Proceedings of the 3rd ACM on International Workshop on Security And Privacy Analytics*, pp. 31–36. ACM, 2017.
- Chen, C., Seff, A., Kornhauser, A., and Xiao, J. Deepdriving: Learning affordance for direct perception in autonomous driving. In *Proceedings of the IEEE International Conference on Computer Vision*, pp. 2722–2730, 2015.
- Chen, X., Liu, C., Li, B., Lu, K., and Song, D. Targeted backdoor attacks on deep learning systems using data poisoning. *arXiv preprint arXiv:1712.05526*, 2017a.
- Chen, Y., Li, J., Xiao, H., Jin, X., Yan, S., and Feng, J. Dual path networks. In *Advances in Neural Information Processing Systems*, pp. 4467–4475, 2017b.
- Goldstein, T., Studer, C., and Baraniuk, R. A field guide to forward-backward splitting with a fasta implementation. *arXiv preprint arXiv:1411.3406*, 2014.
- Goodfellow, I. J., Shlens, J., and Szegedy, C. Explaining and harnessing adversarial examples. *arXiv preprint arXiv:1412.6572*, 2014.
- Gu, T., Dolan-Gavitt, B., and Garg, S. Badnets: Identifying vulnerabilities in the machine learning model supply chain. *arXiv preprint arXiv:1708.06733*, 2017.
- He, K., Zhang, X., Ren, S., and Sun, J. Deep residual learning for image recognition. In *Proceedings of the IEEE conference on computer vision and pattern recognition*, pp. 770–778, 2016.
- Hu, J., Shen, L., and Sun, G. Squeeze-and-excitation networks. In *Proceedings of the IEEE conference on computer vision and pattern recognition*, pp. 7132–7141, 2018.
- Huang, G., Liu, Z., Van Der Maaten, L., and Weinberger, K. Q. Densely connected convolutional networks. In *Proceedings of the IEEE conference on computer vision and pattern recognition*, pp. 4700–4708, 2017.
- Kingma, D. P. and Ba, J. Adam: A method for stochastic optimization. *arXiv preprint arXiv:1412.6980*, 2014.
- Liu, Y., Ma, S., Aafer, Y., Lee, W.-C., Zhai, J., Wang, W., and Zhang, X. Trojaning attack on neural networks. 2017.
- Mei, S. and Zhu, X. Using machine teaching to identify optimal training-set attacks on machine learners. In *Twenty-Ninth AAAI Conference on Artificial Intelligence*, 2015.
- Nelson, B., Barreno, M., Chi, F. J., Joseph, A. D., Rubinstein, B. I., Saini, U., Sutton, C. A., Tygar, J. D., and Xia, K. Exploiting machine learning to subvert your spam filter. *LEET*, 8:1–9, 2008.
- Ozuysal, M., Lepetit, V., and Fua, P. Pose estimation for category specific multiview object localization. In *2009 IEEE Conference on Computer Vision and Pattern Recognition*, pp. 778–785. IEEE, 2009.

- Parkhi, O. M., Vedaldi, A., Zisserman, A., et al. Deep face recognition. In *bmvc*, volume 1, pp. 6, 2015.
- Sandler, M., Howard, A., Zhu, M., Zhmoginov, A., and Chen, L.-C. Mobilenetv2: Inverted residuals and linear bottlenecks. In *Proceedings of the IEEE Conference on Computer Vision and Pattern Recognition*, pp. 4510–4520, 2018.
- Shafahi, A., Huang, W. R., Najibi, M., Suciu, O., Studer, C., Dumitras, T., and Goldstein, T. Poison frogs! targeted clean-label poisoning attacks on neural networks. In *Advances in Neural Information Processing Systems*, pp. 6103–6113, 2018.
- Suciu, O., Marginean, R., Kaya, Y., Daume III, H., and Dumitras, T. When does machine learning {FAIL}? generalized transferability for evasion and poisoning attacks. In *27th {USENIX} Security Symposium ({USENIX} Security 18)*, pp. 1299–1316, 2018.
- Sun, Y., Wang, X., and Tang, X. Deep learning face representation from predicting 10,000 classes. In *Proceedings of the IEEE conference on computer vision and pattern recognition*, pp. 1891–1898, 2014.
- Szegedy, C., Zaremba, W., Sutskever, I., Bruna, J., Erhan, D., Goodfellow, I., and Fergus, R. Intriguing properties of neural networks. *arXiv preprint arXiv:1312.6199*, 2013.
- Szegedy, C., Liu, W., Jia, Y., Sermanet, P., Reed, S., Anguelov, D., Erhan, D., Vanhoucke, V., and Rabinovich, A. Going deeper with convolutions. In *Proceedings of the IEEE conference on computer vision and pattern recognition*, pp. 1–9, 2015.
- Turner, A., Tsipras, D., and Madry, A. Clean-label backdoor attacks. 2018.
- Wang, R., Han, C., Wu, Y., and Guo, T. Fingerprint classification based on depth neural network. *arXiv preprint arXiv:1409.5188*, 2014.
- Xiao, H., Xiao, H., and Eckert, C. Adversarial label flips attack on support vector machines. In *ECAI*, pp. 870–875, 2012.
- Xie, S., Girshick, R., Dollár, P., Tu, Z., and He, K. Aggregated residual transformations for deep neural networks. In *Proceedings of the IEEE conference on computer vision and pattern recognition*, pp. 1492–1500, 2017.
- Zhu, C., Huang, W. R., Shafahi, A., Li, H., Taylor, G., Studer, C., and Goldstein, T. Transferable clean-label poisoning attacks on deep neural nets. *arXiv preprint arXiv:1905.05897*, 2019.

A. Coefficients Optimization Step in Convex Polytope

Algorithm 1 Convex Polytope - Coefficients Updating

```

1: Input:  $A \leftarrow \{\phi(x_p^{(j)})\}_{j=1}^k$ 
2:  $\alpha \leftarrow \frac{1}{\|A^T A\|}$ 
3: for  $i = 1$  to  $m$  do
4:   while not converged do
5:      $\hat{c}^{(i)} \leftarrow c^{(i)} - \alpha A^T (A c^{(i)} - \phi^{(i)}(x_t))$ 
6:     if  $\text{loss}(\hat{c}^{(i)}) \geq \text{loss}(c^{(i)})$  then
7:        $\alpha \leftarrow \frac{1}{\alpha}$ 
8:     else
9:        $c^{(i)} \leftarrow \hat{c}^{(i)}$ 
10:    project  $c^{(i)}$  onto the probability simplex.
11:   end if
12: end while
13: end for

```

In each iteration, Convex Polytope performs three steps. We observed that step one takes significant amount of time compared to the other two steps. Algorithm 1 shows the details of step one, which searches for the (most) suitable coefficients for the current poisons at the time.

B. Single-Target Mode

B.1. Linear Transfer Learning

Figure 13 shows the attack success rates of CP, BP, BP-3x and BP-5x, against each individual victim model.

B.2. End-to-End Training

Figure 14 shows the attack success rates of CP, BP, BP-3x and BP-5x, against each individual victim model end-to-end training victims. Among them, the last row presents the black-box setting. We note that none of CP, BP, and BP-3x shows attack transferability for GoogLeNet. (Zhu et al., 2019) has made a similar observation. They argued that since GoogLeNet has a more different architecture than the substitute models, it is more difficult for the “attack zone” to survive end-to-end training.

B.3. Effectiveness of Bullseye Idea

Figure 15 shows the attack success rates of BP and the other nine alternatives, which are described at Section bullseye-effectiveness.

C. Implementation Details

Convex Polytope authors released the source code of CP along with the substitute networks.⁶ We used their implementation directly for comparison. For all experiments, we use PyTorch-v1.3.1 over Cuda 10.1. We run all the attacks using NVIDIA Titan RTX graphics cards. For solving Eq. 1 (Convex Polytope) and Eq. 3 (Bullseye Polytope), we used the similar settings and parameters to what is practiced by (Zhu et al., 2019).

⁶All models are trained with the same architecture and hyper-parameters defined in <https://github.com/kuangliu/>, except for dropout.

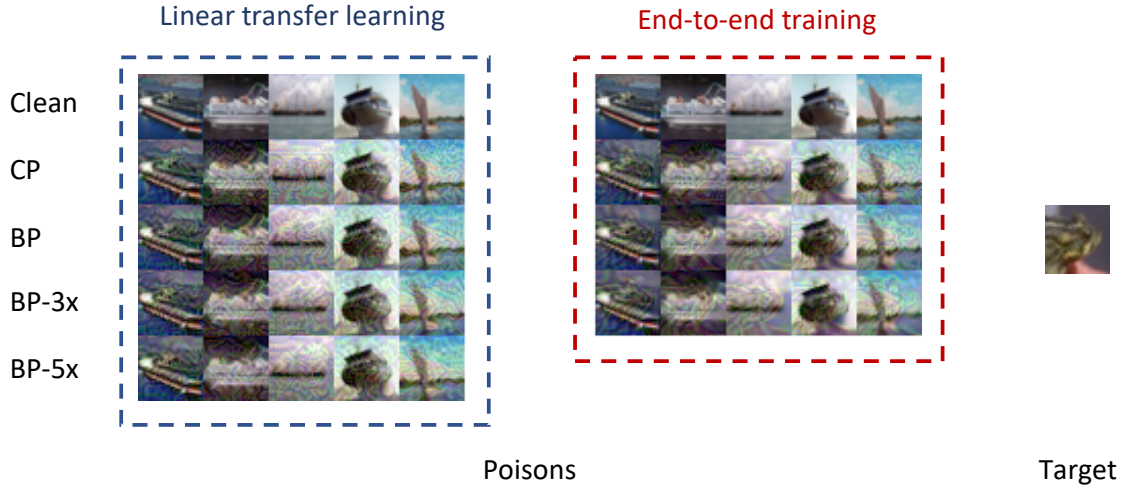


Figure 12. Poisons crafted by Convex Polytope and Bullseye Polytope attacks. First row shows the original images selected for crafting the poisons.

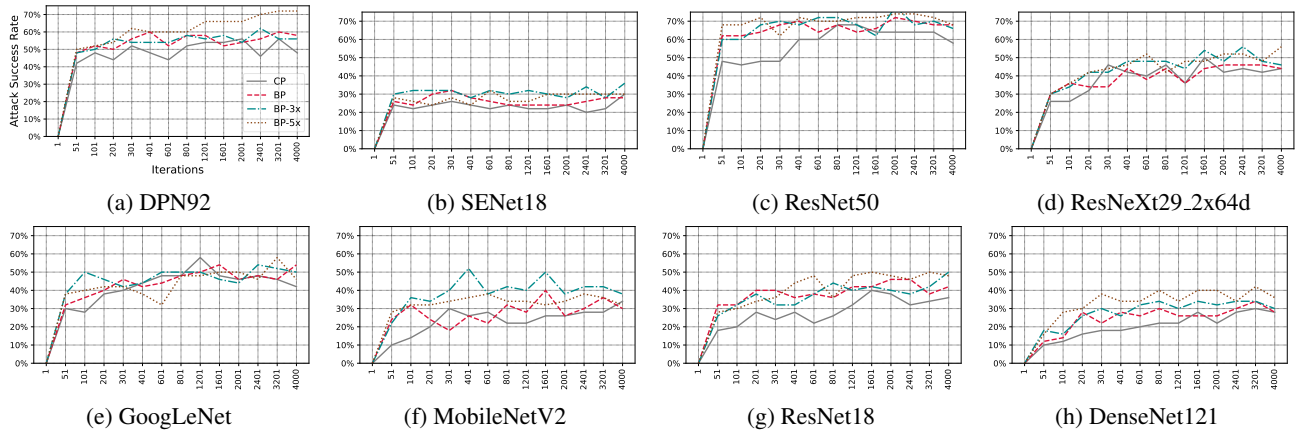


Figure 13. Linear transfer learning: Success rates of CP, BP, BP-3x and BP-5x, against each individual victim model.

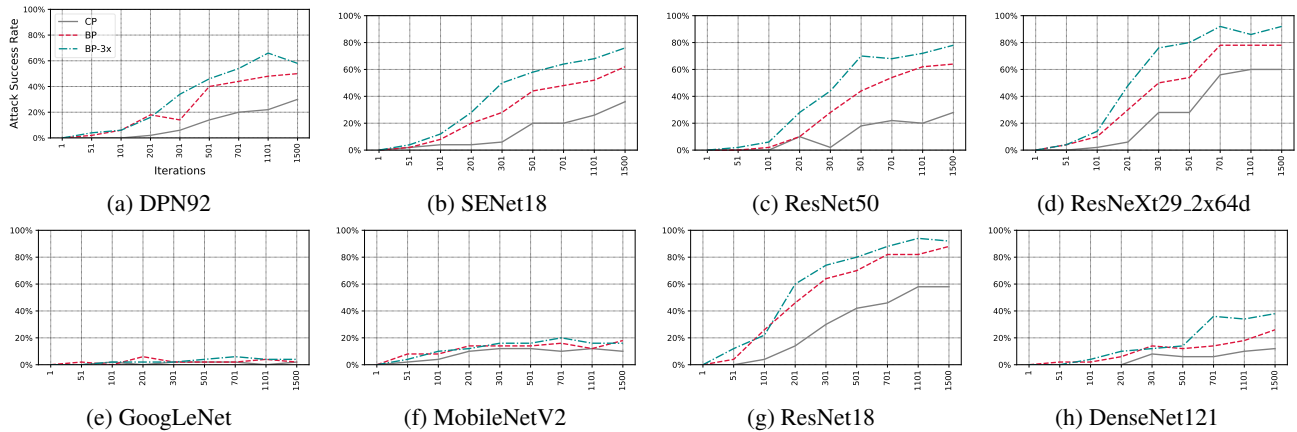


Figure 14. End-to-end training: Success rates of CP, BP, BP-3x and BP-5x, against each individual victim model. Notice GoogLeNet, MobileNetV2, ResNet18 and DenseNet121 are the black-box setting.

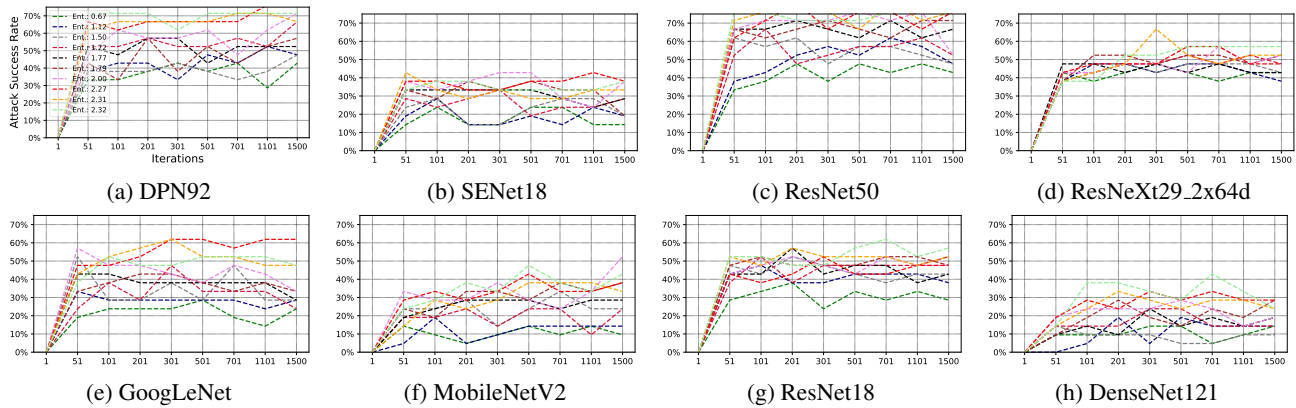


Figure 15. Linear transfer learning: Success rates of BP and the other nine alternatives described at Section 6.1.4, against each individual victim model.

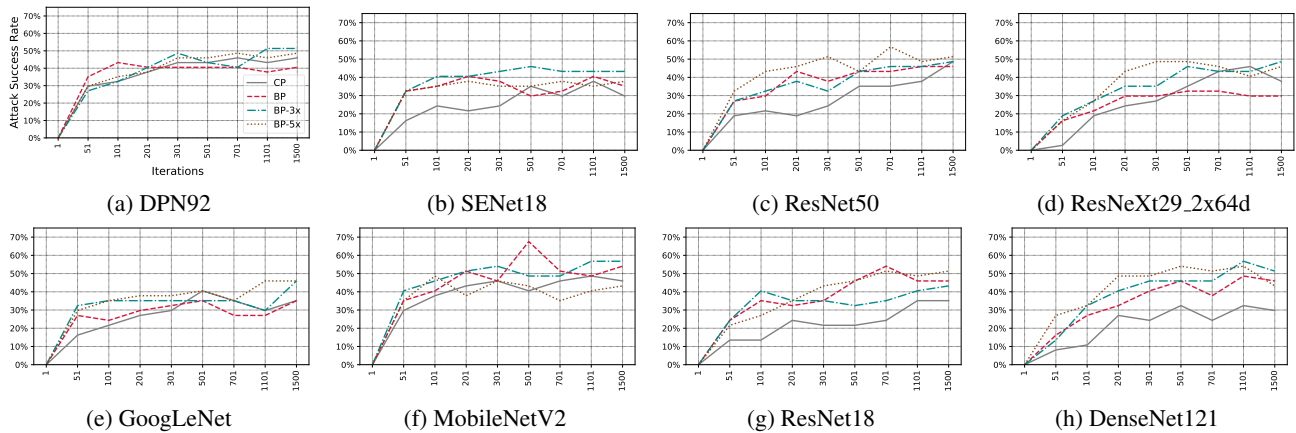


Figure 16. Linear transfer learning when we have 50% overlap between the training sets of substitute and victim’s networks: Success rates of CP, BP and BP-3x, against each individual victim model.

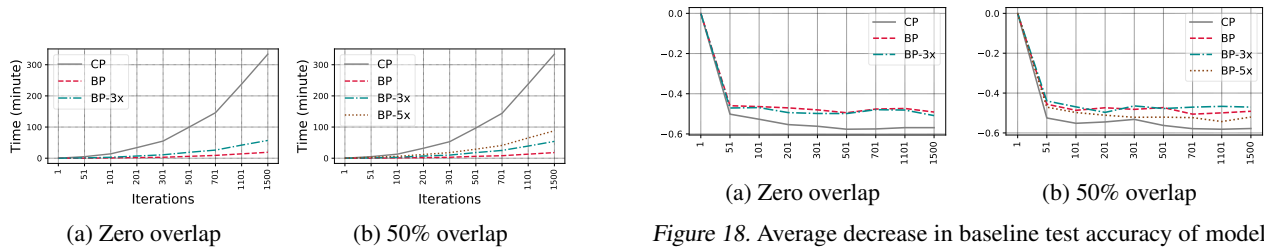


Figure 17. Attack execution time.

Figure 18. Average decrease in baseline test accuracy of models in linear transfer learning settings, when there is zero or 50% overlap between training sets of the substitute networks and victim’s network.